Since January 2020 Elsevier has created a COVID-19 resource centre with free information in English and Mandarin on the novel coronavirus COVID-19. The COVID-19 resource centre is hosted on Elsevier Connect, the company's public news and information website.

Veterinary Microbiology 242 (2020) 108579

Contents lists available at ScienceDirect

Veterinary Microbiology

journal homepage: www.elsevier.com/locate/vetmic

A novel low virulent respiratory *infectious bronchitis virus* originating from the recombination of QX, TW and 4/91 genotype strains in China

Mengjiao Huang[a], Chuangchao Zou[a], Yuan Liu[a], Zhenling Han[a], Chunyi Xue[b,*], Yongchang Cao[b,*]

[a] State Key Laboratory of Biocontrol, School of Life Sciences, Sun Yat-sen University, Guangzhou 510006, China
[b] School of Life Science, Sun Yat-sen University, Higher Education Mega Center, Guangzhou, 510006, China

ARTICLE INFO

Keywords:
Infectious bronchitis virus
Recombination
QX genotype
TW genotype
4/91 genotype

ABSTRACT

In China, variants of *infectious bronchitis virus* (IBV) evolve continually and diverse recombinant strains have been reported. Here, an IBV strain, designated as ck/CH/LJX/2017/07 (referred as JX17) was isolated from chicken vaccinated with H120 and 4/91 in Jiangxi, China, in 2017. Sequence analysis reveals of the S1 gene of JX17 the highest nucleotide identity of 98.15% with that of GI-7 genotype TW2575/98 strain. Furthermore, whole genome analysis among JX17 and other 18 IBV strains demonstrates that JX17 has the highest nucleotide identity of 95.94% with GI-19 genotype YX10 strain. Among all genes of JX17 except the S1 gene, the N gene and 3' UTR have the highest identity to GI-13 genotype 4/91 strain and the rest genes are the most identical to GI-19 genotype YX10 strain. Analyzed by the RDP and SimPlot, the recombination of JX17 strain was shown to occur in regions which include 5'-terminal S1 gene (20,344 to 22,447 nt), most N gene and 3' UTR (26,163 to 27,648 nt). The pathogenicity study shows that JX17 is a natural low virulent IBV variant which caused respiratory symptoms but no death. Taken together, these results indicate that IBV strains continue to evolve through genetic recombination and three prevalent genotypes in China including QX, TW and 4/91 have started to recombine.

1. Introduction

Infectious bronchitis virus (IBV) is the positive-sense single-stranded RNA virus and the causative agent of a highly contagious respiratory disease of major economic importance to the poultry industry (Cook et al., 2012). Similar to other coronavirus, the genome of IBV contains 6 genes (Sawicki and Sawicki, 1998). The spike (S) glycoprotein, encoded by gene 2, is cleaved into S1 and S2 submits by cellular proteases upon viral invasion, with S1 forming the tip of a spike and S2 anchoring to the viral membrane(Cavanagh et al., 1992). The S1 subunit, with virus neutralizing epitopes, plays an important role in viral attachment to host cells (Cavanagh, 1983). Both of envelope protein (E) and membrane glycoprotein (M), encoded by gene 3 and gene 4 individually, are membrane-binding proteins. The nucleocapsid protein (N), encoded by gene 6, plays a key role in viral replication and assembly as well as in cellular immunity (Ignjatovic and Galli, 1995). At the same time, there are other genes that encode for proteins interspersed among structural genes, namely 3a, 3b, 5a, and 5b (Boursnell et al., 1987).In addition to these conventional protein, non-structural proteins such as 4b, 4c, and 6b, were found to exist in most IBVs and Turkey coronavirus (TCoV) (Gomaa et al., 2008; Reddy et al., 2015; Thor et al., 2011).

In China, IBV strains have been identified since 1982 and then struck the whole country (Han et al., 2011). In previous studies, the S1 gene phylogenetic analysis indicated that IBV strains isolated in China could be divided into at least 7 genotypes including QX-type (GI-19), TW-type (GI-7), 4/91-type (GI-13), Mass-type (GI-1), HN08-type (GI-22), TC07-2-type (GVI-1) and LDT3-type (Feng et al., 2017; Li et al., 2010; Xu et al., 2018). QX (GI-19) genotype strains, first isolated from Qingdao, China in 1996, are dominant epidemic strains in China at present (Xu et al., 2018). Recently, the prevalence of TW genotype strains, found in Taiwan, China, starts to exacerbate in mainland China (Feng et al., 2017). IBV strains isolated in Taiwan were divided into TW-I and TW-II genotypes, both of which were grouped into GI-7, with the former isolated frequently in mainland China commonly exhibiting nephrogenic, and the later isolated in Taiwan before 1990s usually presenting with respiratory symptoms (Wang and Huang, 2000; Wang and Tsai, 1996). Another widely prevalent genotype in China, the 793/B (4/91) type (GI-13), which first emerged in Europe in 1991 and quickly spread around the world (Cook et al., 1996), is easy to recombine with other strains in China (Liu et al., 2013; Zhang et al.,

* Corresponding authors.
E-mail addresses: xuechy@mail.sysu.edu.cn (C. Xue), caoych@mail.sysu.edu.cn (Y. Cao).

https://doi.org/10.1016/j.vetmic.2020.108579
Received 12 November 2019; Received in revised form 8 January 2020; Accepted 8 January 2020

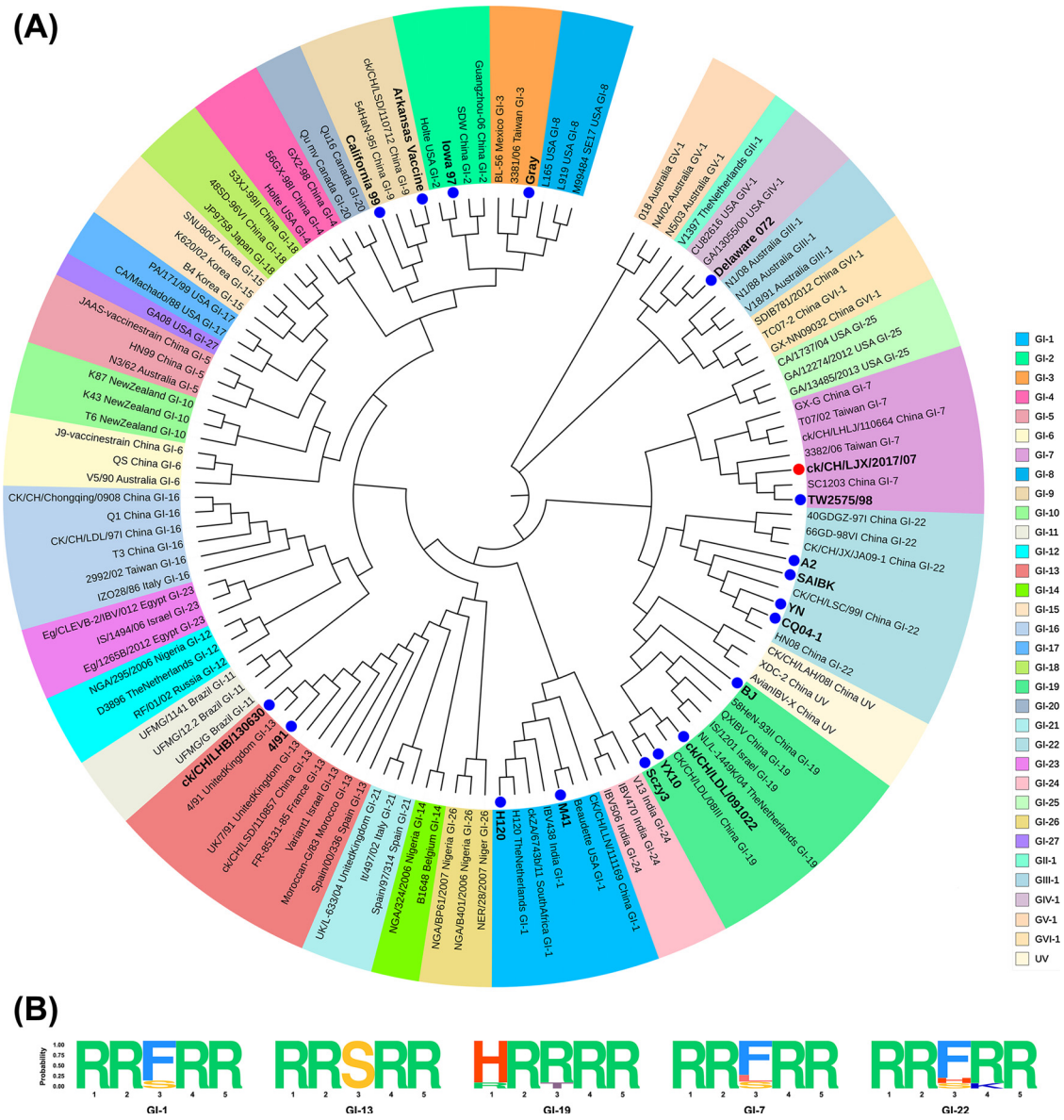

Fig. 1. Consensus phylogenetic tree resulting from the analysis of the S1 gene of JX17 (red dots) and 122 reference strains (A) and spike glycoprotein cleavage recognition motifs of five genotype strains which are epidemic in China (B) (For interpretation of the references to colour in this figure legend, the reader is referred to the web version of this article).

The tree was constructed using the neighbor-joining method with 1000 bootstrap replicates by the MEGA 7.0 software. 122 reference strains include 104 reference strains which were classified into GI-GVI genotypes and 18 strains labeled with blue dots which were used for the complete genome sequence comparison, the phylogenetic analysis and the recombination analysis. Spike glycoprotein cleavage recognition motifs are displayed in sequence logos.

2015).

Owing to the continuous appearance of IBV variants with possible shift of the serotype or pathogenicity, IB breaks out frequently even among the vaccinated flocks (Jackwood, 2012). SAIBK variant, presenting as nephrogenic, was proved to be the recombinant virus of YX10 strain (GI-19), YN strain (GI-19) and Mass-type strain (GI-1) (Yang and Ma, 2013). Coincidentally, variants such as ck/CH/LZJ/111113, originating from ck/CH/LDL/09/022 (GI-19) and 4/91(GI-13), and ck/CH/LHLJ/140906, which presented as a new serotype, originating from 4/91 (GI-13) and H120 (GI-1), were isolated in China (Liu et al., 2013; Zhang et al., 2015). In recent years, the recombinant strains of QX and 4/91 genotype emerged. One typical strain referred as CK/CH/GD/QY16 was isolated in 2016, and then appeared with high frequency (Feng et al., 2018). Additionally, the recombinant viruses involving widespread TW type strains, such as the recombinant of QX and TW I genotype, also began to accumulate (Xu et al., 2016). Nevertheless, the rearrangement of event about all three epidemic genotypes including QX type, TW type and 4/91 type, is unknown. In this study, we sequenced the complete genome of a novel IBV strain JX17 isolated in 2017. By sequence comparison, phylogenetic analysis, and recombination analysis, JX17 was shown to come from QX type, TW type and 4/91 type. An animal experiment was conducted to confirm its pathogenicity. The results of this study present a valuable insight into the evolution of IBV in China, giving a better understanding of the virus at the molecular level.

2. Materials and methods

2.1. Virus isolation and purification

The IBV strain ck/CH/LJX/2017/07 (referred as JX17) was isolated from the IBV-infected yellow feather broilers vaccinated with H120 and

Table 1
Percentage of sequence identities of the complete genome and different regions of JX17 compared with those of other IBV strains (Bold values represent the largest values for each column).

			Gene 1		Gene 2			Gene 3		Gene 4		Gene 5	Gene 6		
strain	genome	5'-UTR	1a	1b	S	S1	S2	3ab	E	M	4bc	5ab	N	6b	3'-UTR
YX10	**95.94**	**99.43**	**97.47**	97.25	88.99	82.28	95.53	99.43	**97.88**	98.15	99.18	94.58	87.97	80.54	97.67
ck/CH/LDL/091022	95.52	98.86	95.95	**97.40**	89.42	82.04	**95.80**	**100.00**	98.48	**97.86**	**99.73**	**98.65**	91.63	79.19	98.95
Sczy3	94.44	99.24	94.98	96.11	89.34	82.10	95.58	98.85	98.18	97.71	93.46	90.74	90.00	80.54	96.25
BJ	90.27	97.34	89.05	93.69	84.39	81.92	86.54	88.51	90.00	93.07	92.64	90.37	90.41	80.54	98.43
A2	90.82	97.15	89.17	93.79	88.39	84.76	92.18	88.51	93.33	92.98	89.37	90.97	89.19	81.18	98.60
YN	90.27	94.11	89.90	91.83	88.83	84.41	92.66	93.10	87.88	93.13	84.69	89.16	87.89	78.75	96.22
SAIBK	89.75	92.97	90.08	90.38	88.51	84.58	92.60	91.38	87.27	91.65	84.81	90.29	87.64	–	96.50
CQ04-1	92.77	97.90	92.61	96.23	89.32	84.47	93.51	93.10	83.98	90.62	85.08	88.94	87.07	78.30	97.18
M41	88.03	95.45	87.31	89.77	85.73	84.68	86.64	83.91	89.09	90.76	88.21	87.81	89.59	–	96.79
H120	88.10	95.16	86.89	89.84	85.79	84.56	86.85	84.48	87.88	90.91	86.30	90.29	91.71	75.88	97.93
TW2575/98	88.93	95.15	86.47	90.12	**94.63**	**98.15**	91.59	84.48	89.39	91.94	84.11	88.26	88.46	81.88	90.36
ck/CH/LHB/130630	88.13	94.40	86.71	89.33	84.26	81.37	86.75	84.48	84.18	91.82	87.12	89.16	97.32	100.00	99.47
4/91	88.17	94.40	86.73	89.40	84.26	81.43	86.70	84.48	84.18	91.82	87.12	89.16	**97.40**	**100.00**	**99.65**
Gray	88.40	95.54	87.61	89.82	85.49	82.86	87.78	85.63	88.07	91.57	87.67	88.71	90.05	94.46	86.00
Iowa_97	88.30	95.73	87.45	90.09	84.71	82.61	86.54	82.76	88.99	90.45	86.85	88.94	89.59	94.22	93.60
California_99	88.11	95.34	87.02	89.82	84.62	81.49	87.33	83.33	88.48	91.94	87.67	89.62	91.95	83.08	96.42
Arkansas_Vaccine	88.29	93.64	87.16	89.96	85.22	82.29	87.76	85.63	87.46	92.06	87.67	89.39	90.98	94.67	95.51
Delaware_072	86.96	95.54	86.84	89.87	76.55	72.22	80.18	83.33	86.97	90.32	86.30	89.39	90.24	94.67	96.23

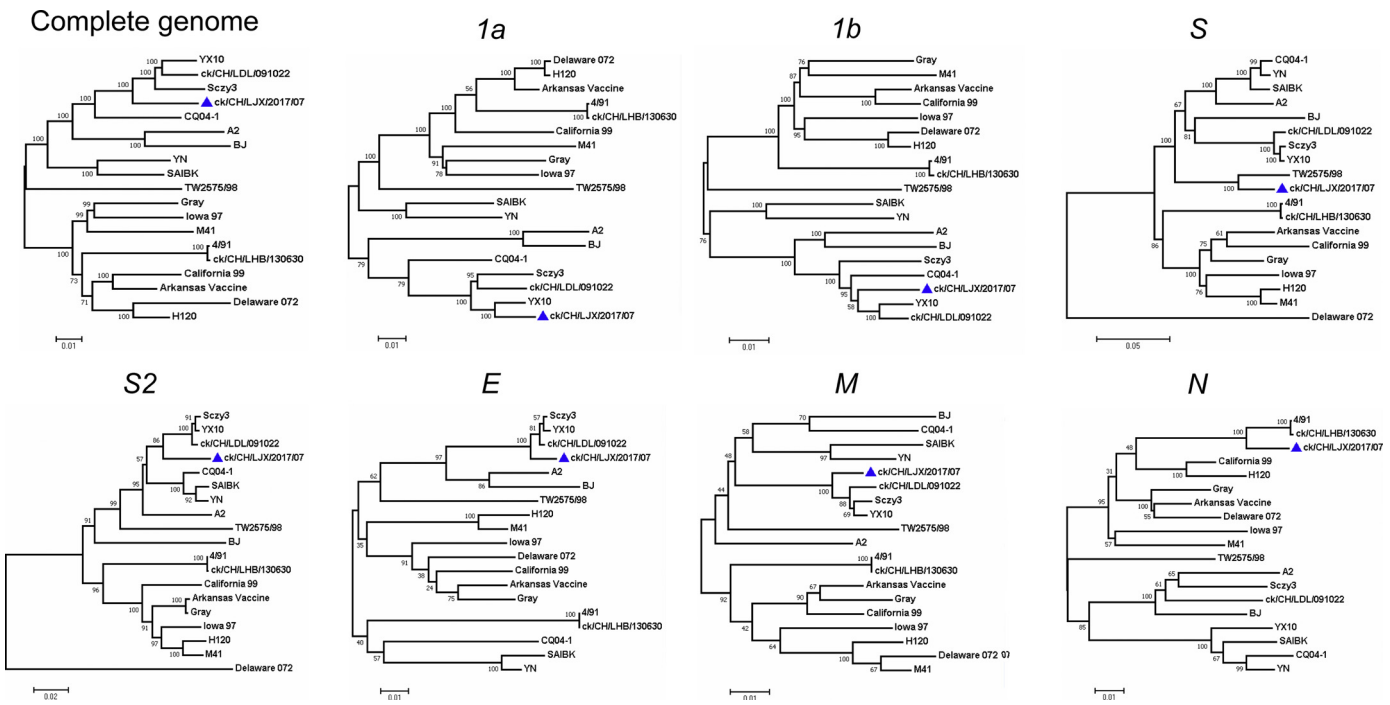

Fig. 2. Phylogenetic trees based on the complete genome and specific genes of the strains.
Phylogenetic trees were constructed using the neighbor-joining method (bootstrapping for 1000 replicates). The JX17 sequence is labeled with blue triangle.

4/91 strains in Jiangxi province, China, in November 2017. The infected chickens appeared typical signs of IBV infection, such as coughing, sneezing, gasping, tracheal rale and wet droppings. The viruses were propagated through blind passage five times in 9-day-old embryos of specific pathogen-free (SPF) chickens via the allantoic cavity. The allantoic fluid was examined using RT-PCR to detect the virus with PrimerScript™ One Step RT-PCR Kit Ver.2 (TaKaRa, Japan) according to the manufacturer's instruction. PCR primers for IBV detection were described before (Zhang et al., 2018). Furthermore, we used limiting dilution passage which was described before to get monocle IBV virus (Zhang et al., 2018). Briefly, 0.2 ml allantoic fluid diluted to 10^2-10^9 times was inoculated into each embryo (4 embryos for each dilution). The allantoic fluid from the embryos inoculated with the highest dilution ratio that was positive for IBV was used for the next dilution passage. After three limiting dilution passages, the allantoic fluid positive for IBV was selected for genome sequencing and pathogenicity test. The virus isolation and follow-up experiments were carried out in biosafety level 2 laboratory.

2.2. Viral RNA extraction and high-throughput sequencing

IBV was enriched for 100 folds by ultracentrifugation and purified by sucrose density gradient centrifugation. The complete genome sequence of JX17 was sequenced and assembled as described previously (Gong et al., 2017). Briefly, total RNA was extracted using TRIzol Reagent (Invitrogen Life Technologies, Grand Island, NY, USA) and the ribosomal RNA was eliminated with the Ribo-Zero rRNA Removal Kit (Illumina, San Diego, CA, USA) according to the manufacturer's

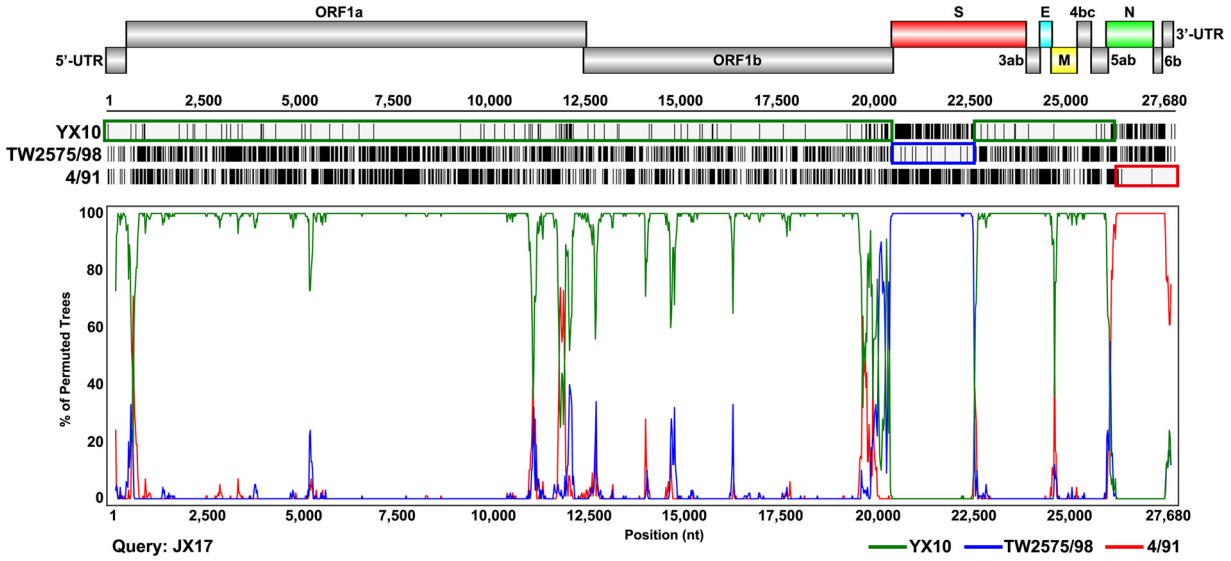

Fig. 3. BootScan analysis of the genome of JX17 strain.
IBV strains YX10 (green), TW2575/98 (blue) and 4/91 (red) were used as putative parental strains, while JX17 strain was used as the query strain. The y-axis shows the percentage of permutated trees using a sliding window of 200-bp width centered on the plotted position, with a step size of 20 bp. The genome map is shown at the top of the figure. Sequence comparison of YX10, TW2575 and 4/91 was performed using Geneious 9.1.4 with JX17 as the reference strain. The boxes of different colors indicate the most similar region of three putative parental strains to JX17 strain.

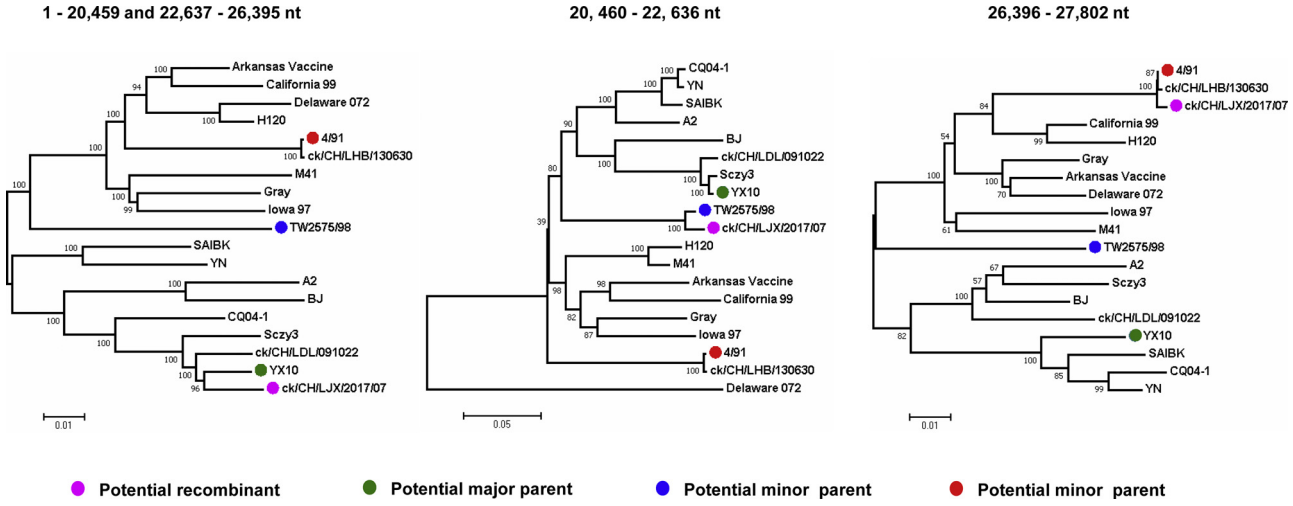

Fig. 4. Phylogenetic trees of different genome regions among JX17, YX10, TW2575/98, 4/91 and other 15 reference strains.
Phylogenetic trees were constructed using the neighbor-joining method (bootstrapping for replicates). The recombinant strain JX17 is labeled with purple dot, the major parental strain YX10 with green dot, the minor parental strain TW2575/98 with blue dot and the minor parental strain 4/91 with red dot.

instructions. After RT-PCR with random primers, we performed 150-bp paired-end shotgun metatranscriptome sequencing on the cDNA libraries by using an Illumina HiSeq system. The short reads are assembled by *de novo* following filtering out the host sequence. The genome sequence of JX17 have been deposited in the GenBank database under the accession number of MN307884.

2.3. Sequence comparison and phylogenetic analysis

The S1 gene sequences of JX17 and 122 reference strains were aligned using the ClustalW multiple alignment algorithm. The S1 gene sequences of 104 reference strains, which represented the well-established genotypes (GI (1-27) - GVI) as described before (Valastro et al., 2016), were retrieved from the GenBank database. The S1 gene sequences of 18 strains whose genome sequences were uploaded in NCBI were also included in the alignment. Comparison and analysis of specific gene sequences and complete genome were conducted using EditSeq and MegAlign programs in the Lasergene package (DNAStar, Madison, WI). Phylogenetic trees were constructed by the neighbor-joining method with 1000 bootstrap replicates with MEGA version 7.0 software.

2.4. Recombination analysis

The potential within-gene recombination events in JX17 were analyzed with the Recombination Detection Program 4 (RDP4, version 4.94), which implements seven detection methods including RDP, GENECONV, BootScan, MaxChi, Chimaera, SiScan and 3Seq. Potential recombination events and breakpoints were further verified by Simplot and BootScan analyses with SimPlot Program (version 3.5.1). The nucleotide identity comparison was carried out using the Kimura (2-parameter) method with a transition-transversion ratio of 2, and the window width and step size were 200 and 20 bp, respectively. BootScan was carried out using the neighbor-joining method with 100 replicates.

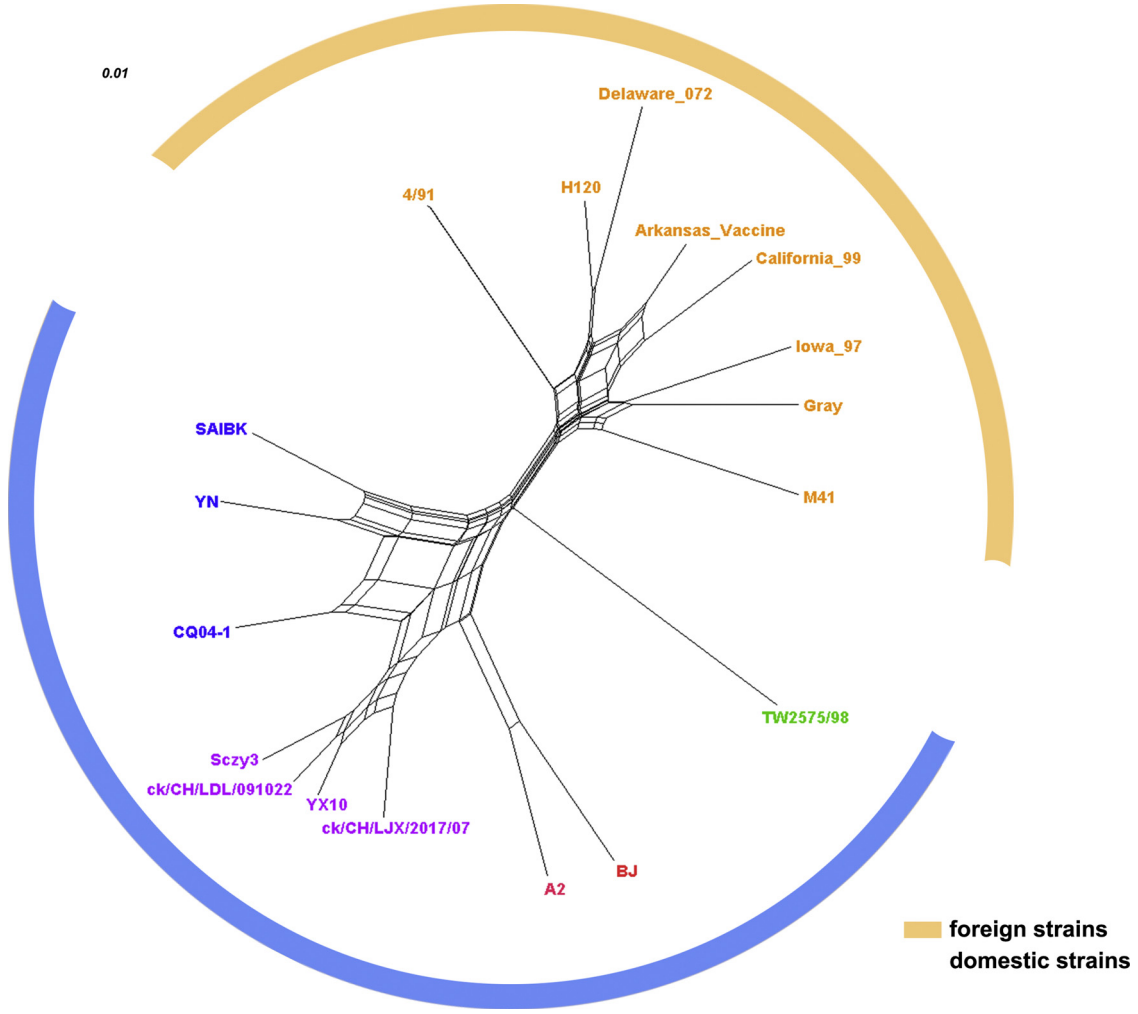

Fig. 5. Recombination networks among 18 IBV strains.
Recombination networks from nucleotide sequence alignments on complete genomes of 18 IBV strains were generated using SplitsTree 4.14.5. The multiple reticulate networks indicate the recombination events among IBV strains. A bar indicates the sequence substitutions per site. The phi test did find statistically significant evidence for recombination in complete genome ($P < 0.001$). Strains isolated in China are clustered on one side and foreign strains are clustered on the other side, covered by blue and yellow arcs respectively.

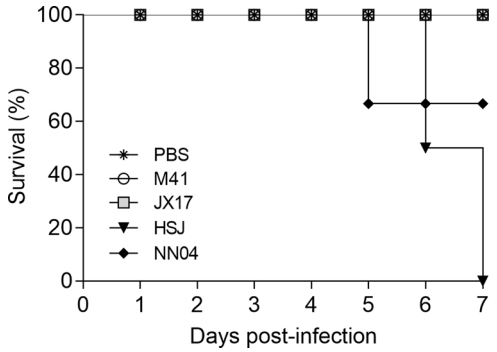

Fig. 6. Survival rates of chickens challenged with IBV JX17, M41, HSJ and NN04 strains.
The mortality of chicken in each group was recorded from 1 to 7 dpi.

Recombination networks on alignments of JX17 and 17 reference strains' genomes (ck/CH/LHB/130630 strain was removed because it may be the re-isolated 4/91 vaccine strain) were performed by SplitsTree 4.14.5 (Huson, 1998). Statistical analysis of the recombination networks was generated by the Phi test.

2.5. Pathogenicity test

Animal experiments were performed in accordance with the guidelines of Sun Yat-Sen University Institutional Animal Care and Use Committee. Seventy-five 7-day-old SPF chickens were divided into five groups equally and kept in 5 isolators. Each chicken in the infected group was infected with $10^{5.0}$ EID_{50} of JX17, M41, HSJ and NN04 strains respectively by the oculonasal administration, while PBS was given as negative control. M41, HSJ and NN04 strains under the accession number of DQ834384.1, MG544176.1 and CQ265951.1 were kept in our laboratory. The chickens were monitored daily for 7 days after the challenge. Five chickens from each group were euthanized 3 days post infection (dpi), and the remaining chickens were euthanized at 7 dpi for autopsy. The trachea and kidney tissues were harvested integrally for hematoxylin and eosin (HE) stain and the detection of virus loads.

2.6. Histopathology

The trachea and kidney tissues collected at 7 dpi were fixed in 10% neutral formalin for 48 h at room temperature. Fixed samples were processed routinely, embedded in paraffin wax, cut into 5 μm-thin sections and stained with hematoxylin and eosin. The slides were

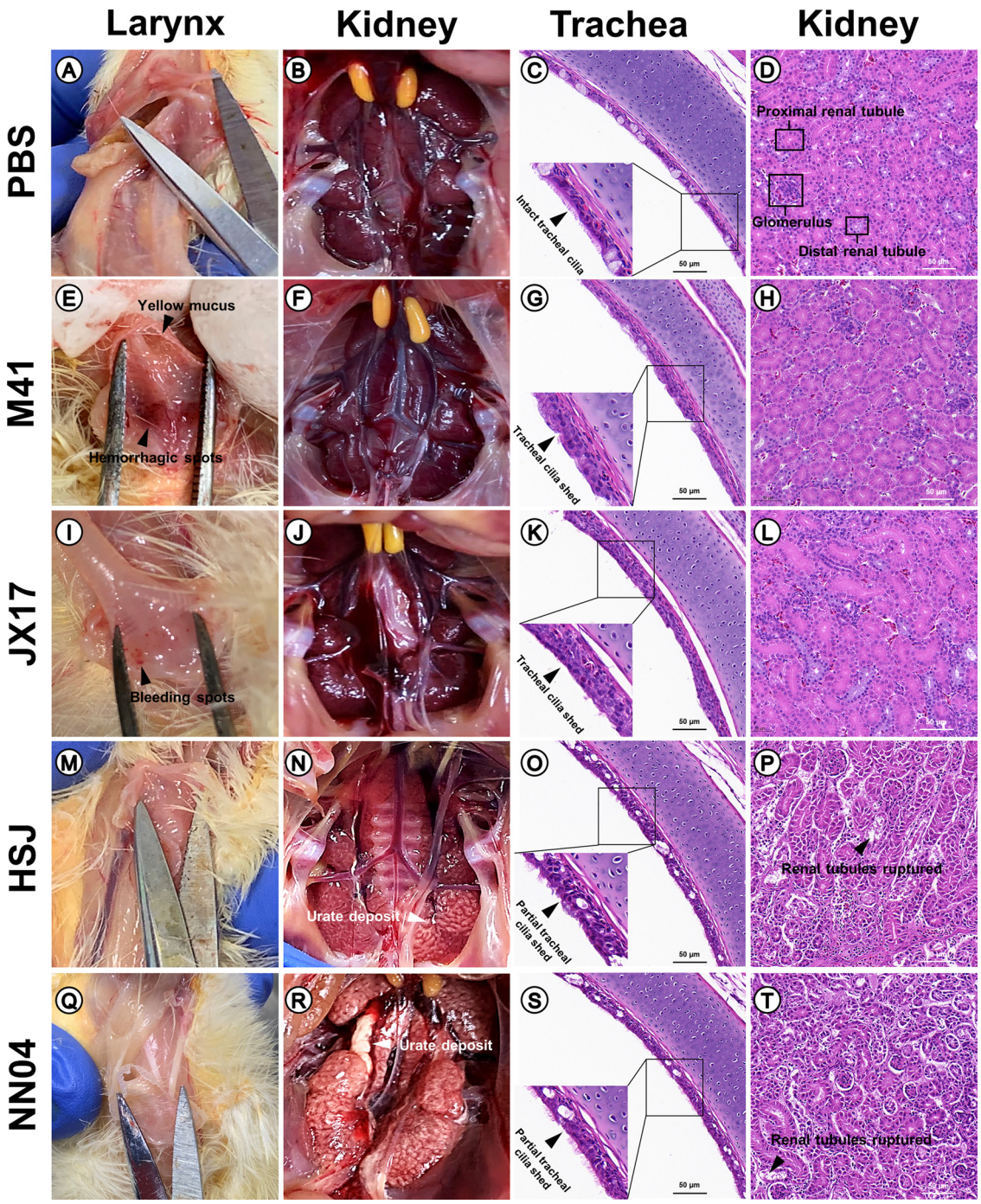

Fig. 7. Gross and histopathologic lesions in trachea and kidney from chickens 7 days post infection.
Chickens (n = 10) were sacrificed at 7 dpi, and the tracheas and kidneys were collected for histological analysis. Larynx and kidney autopsy in each group were shown in figure A, E, I, M, Q and B, F, J, N, R respectively. HE stains of trachea and kidney were shown in figure C, G, K, O, S and D, H, L, P, T respectively. Black and white triangles in Larynx and kidney autopsy indicated the lesion areas. The close-up of the ciliated epithelium was magnified twice in HE stains of trachea. The areas enclosed by black boxes revealed normal distal tubule, proximal tubule and glomerulus in HE stains of kidney in PBS group. Ruptured renal tubules could be observed in HSJ and NN04 group as black triangles indicated.

examined with light microscopy for lesions.

2.7. Inhibition of ciliary activity

When the chickens were euthanized at 3 and 7 dpi, the tracheas were taken out integrally without the mechanical damage and three tracheal rings per chick were prepared. Each ring was placed in a single well of a 96-well plate containing DMEM with 10% (v/v) fetal bovine serum. The movement of the cilia in complete circle region of the trachea ring was observed under the light microscope. To quantify the degree of ciliostasis, the following standard was established for evaluation: 0 indicated that trachea ring did not appear ciliostasis; 1, 2, 3 and 4 indicated that 0–25%, 25–50%, 50–75% and 75–100% of area in trachea ring appeared ciliostasis respectively. An average ciliostasis score was calculated for each group.

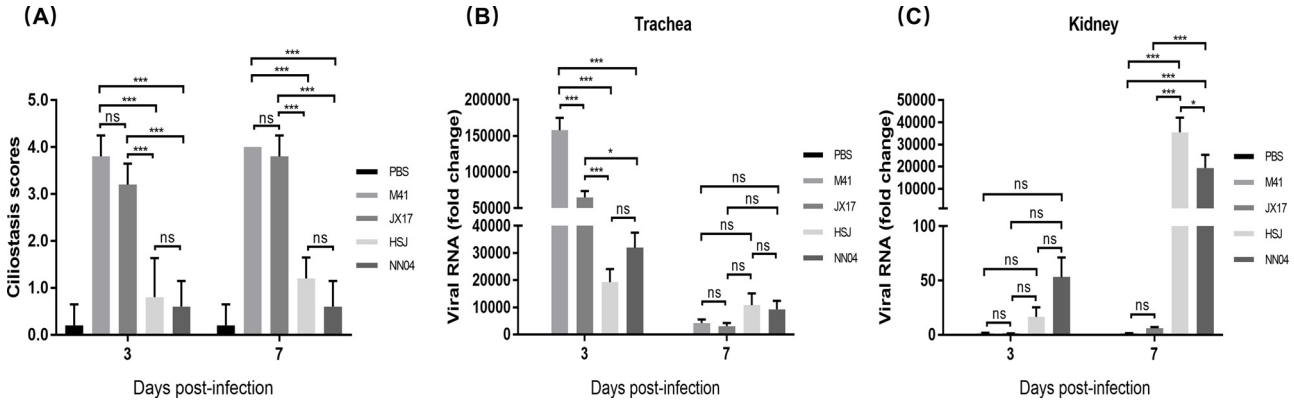

Fig. 8. Tracheal ciliostasis scores (A) and viral RNA in trachea (B) and kidney (C) from chickens challenged with IBV JX17, M41, HSJ and NN04 strains. An average ciliostasis score was calculated for each group. Trachea and kidney were collected to measure the level of viral RNA 3 and 7 dpi respectively. Fold changes were calculated relative to the PBS group and all data are presented as mean ± standard deviation (SD) (n = 5). Statistical significance was considered using two-way ANOVA as follows: *, $P < 0.05$; **, $P < 0.01$; ***, $P < 0.001$; ns, $P > 0.05$.

2.8. Detection of virus loads in trachea and kidney

Total RNA of the trachea and kidney tissues at 3 and 7 dpi were extracted by TRIzol Reagent (Invitrogen Life Technologies) and reverse transcribed using a ReverTra Ace® qPCR RT Master Mix with gDNA Remover kit (TOYOBO, Osaka, Japan). Relative quantitative PCR was performed for the detection of the N gene (Kint et al., 2015) using Hieff™ qPCR SYBR® Green Master Mix (Yeasen, Shanghai, China) on a Light-Cycler 480 PCR system (Roche, Basel, Switzerland), and the *GAPDH* gene was used as the reference gene for normalization (Li et al., 2013). The cycling conditions were as follows: 95 ℃ for 5 min, followed by 40 cycles of 95 ℃ for 10 s, 58 ℃ for 10 s, and 72 ℃ for 30 s, with subsequent incubations at 95 ℃ for 5 s, 60 ℃ for 1 min and 95 ℃ for 15 s. Data were analyzed using the $2^{-\Delta\Delta CT}$ method and presented as the change (n-fold) relative to the control group inoculated with PBS.

2.9. IBV strains published in GenBank

122 representative IBV strains published in GenBank were selected for the phylogenetic analysis of the S1 gene, and 18 IBV strains were used for the complete genome and specific genes (besides the S1 gene) alignment, sequence comparison, phylogenetic, and recombination analysis. The accession numbers of these reference strains are listed in Supplementary Table S1.

3. Results

3.1. Complete genome and organization of JX17 strain

High-throughput sequencing of JX17 genome was performed twice separately and the results were identical. The complete genome of JX17 is comprised of 27,670 nt, excluding poly (A) tail. Gene 1 has 19,893 nt, consisting of ORF1a (11,859 nt) and ORF1b (7959 nt), and it encodes 2 polymerase proteins including 1a and 1b. With a length of 3498 nt, gene 2 has a single ORF and encodes S glycoprotein that is cleaved into S1 and S2 subunits, which are 1620 and 1878 nt (encoding 540 and 625 aa) respectively. Between gene 2 and gene 3, there is only 1 nt overlap. There are 675 nt in gene 3 that encodes 3a and 3b accessory proteins as well as E protein with 174, 189 and 327 nt (encoding 57, 62 and 108 aa) respectively. There are 29 nt overlaps between gene 3 and gene 4. With a length of 1042 nt, gene 4 contains 3 ORFs and encodes M, 4b and 4c proteins which are 675, 285 and 162 nt (encoding 224 aa, 94 aa and 53 aa) respectively. Gene 4 and gene 5 have 4 nt overlaps. Containing 443 nt, gene 5 consists of overlapping 5a and 5b, which are 198 and 249 nt (encoding 65 and 82 aa) respectively. There are 58 nt overlaps between gene 5 and gene 6. Gene 6 encodes N protein and 6b which are 1230 and 198 nt (encoding 409 and 66 aa) respectively. The 5' and 3' UTR of the genome are 525 and 274 nt in length, respectively.

3.2. JX17 strain clusters into GI-7 genotype based on S1 gene

The S1 gene of JX17 is composed of 1620 nt with the nucleotide identity ranges from 62.2 to 98.15% to that of 122 available reference IBV strains. The S1 gene of JX17 has the highest nucleotide identity with that of TW2575/98 (98.15%). The nucleotide identities between the S1 gene of JX17 and those of the vaccine strains used in China including M41, H120 and 4/91 are 83.6%, 83.7% and 79.9%, respectively. As for the S1 gene, JX17 is least like N1/08 Australia strain and the nucleotide identity is only 62.2%. In the phylogenetic tree based on the S1 gene (Fig. 1A), the 122 reference S1 genes are divided into genotypes GI-GVI displayed with different color branches separately. The strain JX17 clusters to the GI-7 genotype (TW-type) that includes reference strains such as TW2575/98 and SC1203.

Furthermore, the motif of the cleavage site of JX17 is Arg-Arg-Phe-Arg-Arg (RRFRR). When virus invades the host, the S protein is cleaved into S1 and S2 subunits by the protease at the cleavage site (Cavanagh et al., 1986) and the motif of the cleavage site is generally comprised of H/S/RRXRR (X for any amino acid). To investigate if there are any relation between cleavage site sequences and genotyping according to the S1 gene, cleavage recognition motifs of 96 sequences clustering to 24 genotypes after removing sequences which lack complete cleavage sequence from 122 reference sequences were analyzed (Fig. S1). In our study, we found that the most dominant motif (RRSRR) is shared by GI-4, GI-5, GI-6, GI-9, GI-12, GI-13, GI-14 and GI-26. Other GI genotypes have the motifs of RRFRR (GI-1, GI-7, GI-22 and GI-24), HRSRR (GI-8) and SRSRR (GI-10). For the QX genotype (GI-19) strains, the motif is HRRRR which is different from that of other GI genotypes. With long distance from GI genotypes in phylogenetic relation, GIII-1, GIV-1, GV-1 and GVI-1 have the motifs of HTRRR, HRRKR, HRKKR and RRIRR. Otherwise, the motifs of GI-1(Mass-type), GI-7(TW-type), GI-13(4/91-type), GI-22(SAIBK-type) prevalent in China is RRFRR, RRFRR, RRSRR and RRFRR respectively (Fig. 1B). The motif of JX17 is typical RRFRR of TW-type.

3.3. Genome sequence comparison and phylogenetic analysis of JX17 strain

The genome of JX17 and 18 IBV reference strains was compared. As shown in Table 1, the sequence comparison analysis reveals that the genome nucleotide identity between JX17 and these strains ranges from 86.96 to 95.94%. JX17 has the highest resemblance to YX10 with 95.94% identity and is least similar to Delaware 072 with 86.96% identity. As for specific genes, the nucleotide identity of the 5'-UTR, 1a,

1b, S, S1, S2, 3ab, E, M, 4bc, 5ab, N, 6b, and the 3'-UTR between JX17 and other IBV strains were 92.97 to 99.43%, 86.47 to 97.47%, 89.33 to 97.40%, 76.55 to 94.63%, 72.22 to 98.15%, 80.18 to 95.80%, 82.76 to 100%, 83.98 to 97.88%, 90.32 to 97.86%, 84.11 to 99.73%, 87.81 to 98.65%, 87.07 to 97.40%, 31.46 to 100% and 86.00 to 99.65%, respectively. JX17 has the highest nucleotide identity with QX strain YX10 in most of their genes (5'-UTR, 1a, 1b, S2, 3ab, E, M, 4bc and 5ab). In terms of the N, 6b, and 3'-UTR gene, JX17 is most similar to the strain 4/91. With regard to the S1 or full S gene, it has the highest identity with the strain TW 2575/98 (98.15% or 94.63%).

In order to assess the genetic relatedness between JX17 and the reference IBV strains, phylogenetic trees were constructed for the nucleotide sequences of the complete genome and specific genes. As shown in Fig. 2, the complete genome, 1a, 1b, S2, E, M of JX17 is in the same cluster as those of YX10, whereas the full S gene, similar to the S1 gene, is located in the cluster of TW strain. In addition, the N gene is in 4/91 branch and evolutionarily distant from QX branch. To sum up the results of the sequence comparison and phylogenetic analysis, it is reasonable to assume that JX17 has a close evolutionary relationship with YX10, TW and 4/91.

3.4. JX17 strain originated from recombination

In order to detect possible recombination events within the JX17 genomic sequence, RDP analysis was conducted and the genomes of 18 reference strains were used as putative parent strains. The results indicate that JX17 is possibly a recombinant strain formed by a major parent strain YX10 and two minor parent strains TW and 4/91. It has been proved that the recombination breakpoints of JX17 are located at the 20,344 to 22,447 and 26,163 to 27,648 nt. The region 1 to 20,343 and 22,448 to 26,162 nt is 97.5% similar to YX10, the region 20,344 to 22,447 nt shows 98.1% similarity with TW2575/98, and the region 26,163 to 27,648 nt shows 99.8% similarity with 4/91. The P-value of RDP method is 2.828×10^{-252} and 2.784×10^{-151}. To confirm the results of the RDP analysis, genomic sequence analysis of JX17, YX10, TW and 4/91 was carried out using the Simplot software. The Simplot result indicates that there is recombination signal. Recombination diagram is shown by BootScan analysis in SimPlot software (Fig. 3). The recombination region consists of 5'-terminal S1 protein gene with 2104 nt, partial N protein gene and 3'UTR with 1485 nt. At the same time, the phylogenetic trees of three detected recombinant regions including 1 to 20,459 and 22,637 to 26,395 nt, 20,460 to 22,636 nt and 26,396 to 27,802 nt among the 19 strains were constructed after alignment (Fig. 4). It demonstrates that there is a topological alternation in the recombinant region of JX17, which further confirms the recombination event.

Recombination network analysis of the whole genome of JX17 and 17 reference IBV strains were performed (Fig. 5). A total of 6581 informative sites were found in the genome of the 18 IBV strains, and the phi test presented statistically significant evidence for recombination ($P < 0.001$). The recombination of domestic and foreign strains shows a long distance, and domestic epidemic strains recombine frequently.

3.5. JX17 strain is low virulent and causes the respiratory signs

All the chickens were observed for clinical signs after the challenge. Chickens in M41 and JX17 groups showed symptoms of nasal and ocular discharge, increased drinking water and coughing whereas HSJ and NN04 groups with depressed spirit and weak activity. None of the chickens in the PBS group showed any clinical signs. As for the survival rate after challenge shown in Fig. 6, JX17 and M41 cause no death from 1 to 7 dpi. However, NN04 and HSJ can cause death with mortality rates of 30% and 100%, which belong to 4/91 genotype and QX genotype respectively(Li et al., 2010; Zhang et al., 2018).

In the JX17-challenged chickens, the autopsy showed minor bleeding spots in the larynx, but no obvious symptoms of urate deposition in the kidney (Fig. 7I & J). The M41-challenged chickens appeared not just hemorrhagic spots but yellow mucus (Fig. 7E). The kidneys in HSJ- and NN04-challenged chickens appeared pale and mottled with urate deposit as white triangles indicated (Fig. 7N & R). Histopathological examination revealed that the ciliated epithelium of the trachea was shed in chickens from JX17 and M41 groups (Fig. 7G & K) while renal tubules were disrupted in chickens from HSJ and NN04 groups (Fig. 7P & T). Inhibition of ciliary activity in the trachea was measured at 3 and 7 dpi (Fig. 8A). Compared to the PBS group, whose ciliostasis score was less than 0.3, M41 and JX17 caused severe tracheal ciliostasis with scores 4.0 ± 0 and 3.8 ± 0.4 respectively at 7 dpi. Furthermore, the virus loads in the trachea and kidney were analyzed at 3 and 7 dpi (Fig. 8B & C). The level of viral RNA of JX17 and M41 was significantly higher than that of HSJ and NN04 in trachea at 3 dpi. The level of viral RNA of HSJ and NN04 was significantly higher than that of JX17 and M41 in kidney at 7 dpi ($P < 0.001$).

4. Discussion

On account of vast territory and climate diversity, the epidemic situation of IB in China, where multiple IBV genotypes and serotypes coexist, is very complex(Liu et al., 2006). IBV variants frequently occurred with diversity, making it more difficult to control this disease (Sjaak et al., 2011). Therefore, it is necessary to analyze the complete genome of some isolated strains to monitor the recombination event. Genome-wide sequences of recombinant IBV strains obtained by Sanger sequencing were reported in previous studies(Chen et al., 2017; Jiang et al., 2017; Wu et al., 2016). In this study, we isolated JX17 strain from yellow feather broilers vaccinated with H120 and 4/91 vaccines and got monocle IBV virus by limiting dilution passages. JX17 was proved to derive from YX10 strain, TW2575/98 strain and 4/91 strain by the recombinant analysis. The pathogenicity test suggests that JX17 strain is a natural low virulent strain appearing as trachea disease.

According to the newly established phylogenetic analysis system based on the S1 gene(Valastro et al., 2016), the recently isolated strain JX17 belongs to the GI-7 genotype, which is widespread in China in recent years (Xu et al., 2018). Previous report showed that the cleavage site motif in the S1 gene is associated with genotype and pathogenicity (Jackwood et al., 2001). RRFRR is in the S1 gene of most TW type strains including JX17 strain. Interestingly, the motif (HRRRR) is only present in GI-19 strains which was firstly isolated in China and prevalent in all world.

By sequence comparison, phylogenetic analysis, and recombination analysis, JX17 was shown to derive from QX strain, TW strain and 4/91 strain. JX17 has the highest nucleotide identity of 95.94% with YX10 strain, which was isolated in Zhejiang province, China, in 2010 (Feng et al., 2015) and reported to be involved in recombinant variants in recent years, such as SAIBK2 (Chen et al., 2017; Jiang et al., 2017; Wu et al., 2016) and QY16 (Feng et al., 2018). TW and 4/91 strains are the minor parent strains of JX17. The 4/91 vaccine strain, the donor of the N gene and 3'UTR to JX17 strain, has been widely used in the global poultry industry. Recent studies revealed that the 4/91 strain has become an important gene donor to variants in genetic evolution of IBV in China (Han et al., 2011; Zhang et al., 2015). Moreover, the typical strain TW2575/98 of TW genotype, the donor of the S1 gene to JX17 strain, were isolated frequently in past few years (Feng et al., 2017). Previous studies found that the recombination hot spots tended to be located in the 1a (nsp2 and nsp3), 1b (nsp16), upstream of the S glycoprotein gene and 3' end of the N gene (Jackwood, 2012). The recombination breakpoints identified in isolate JX17 are located in these genes which include 5'-terminal S1 gene, 3'-terminal N gene and 3' UTR sequence.

The animal experiment, in which chickens appeared mild respiratory signs in JX17 group, contrasts with the survey in the field cases, where obvious respiratory and nephritis signs could be seen. There is a possible reason for this discrepancy: IBV strain JX17 may not

be the only causative pathogen responsible for the occurrence of the outbreak. In addition, TW 2575/98 strain belongs to TW-I genotype which mostly presents nephropathogenic whereas JX17 causes respiratory disease, which indicates although the S1 gene of IBV plays an important role in the viral attachment to host cells, and the induction of neutralizing antibodies, the S1 gene is only a small part of the IBV genome and thus cannot represent all the biological characteristics of the virus.

In conclusion, QX-, TW- and 4/91-type strains have started to recombine, which should be taken into the account. The genomes of emerging mutant strains should be sequenced and the biological characteristics of new strains should be studied to meet the growing challenge of IBV variants.

Funding

This research did not receive any specific grant from funding agencies in the public, commercial, or not-for-profit sectors.

Author contributions

YCC, CYX and MJH conceived and designed the experiments; MJH, YL, ZLH performed the experiments; MJH and CCZ analyzed the data; MJH wrote the paper. YCC and CYX checked and finalized the manuscript. All authors read and approved the final manuscript.

Conflict of interest

The authors declare that they have no conflict interest.

Appendix A. Supplementary data

Supplementary material related to this article can be found, in the online version, at doi:https://doi.org/10.1016/j.vetmic.2020.108579.

References

Boursnell, M.E., Brown, T.D., Foulds, I.J., Green, P.F., Tomley, F.M., Binns, M.M., 1987. Completion of the sequence of the genome of the coronavirus avian infectious bronchitis virus. J. Gen. Virol. 68 (Pt 1), 57–77.

Cavanagh, D., 1983. Coronavirus IBV: structural characterization of the spike protein. J. Gen. Virol. 64 (Pt 12), 2577–2583.

Cavanagh, D., Davis, P.J., Pappin, D.J., Binns, M.M., Boursnell, M.E., Brown, T.D., 1986. Coronavirus IBV: partial amino terminal sequencing of spike polypeptide S2 identifies the sequence Arg-Arg-Phe-Arg-Arg at the cleavage site of the spike precursor propolypeptide of IBV strains Beaudette and M41. Virus Res. 4, 133–143.

Cavanagh, D., Davis, P.J., Cook, J.K., Li, D., Kant, A., Koch, G., 1992. Location of the amino acid differences in the S1 spike glycoprotein subunit of closely related serotypes of infectious bronchitis virus. Avian Pathol. 21, 33–43.

Chen, Y., Jiang, L., Zhao, W., Liu, L., Zhao, Y., Shao, Y., Li, H., Han, Z., Liu, S., 2017. Identification and molecular characterization of a novel serotype infectious bronchitis virus (GI-28) in China. Vet. Microbiol. 198, 108–115.

Cook, J.K., Orbell, S.J., Woods, M.A., Huggins, M.B., 1996. A survey of the presence of a new infectious bronchitis virus designated 4/91 (793B). Vet. Rec. 138, 178–180.

Cook, J.K., Jackwood, M., Jones, R.C., 2012. The long view: 40 years of infectious bronchitis research. Avian Pathol. 41, 239–250.

Feng, K., Xue, Y., Wang, J., Chen, W., Chen, F., Bi, Y., Xie, Q., 2015. Development and efficacy of a novel live-attenuated QX-like nephropathogenic infectious bronchitis virus vaccine in China. VACCINE 33, 1113–1120.

Feng, K., Wang, F., Xue, Y., Zhou, Q., Chen, F., Bi, Y., Xie, Q., 2017. Epidemiology and characterization of avian infectious bronchitis virus strains circulating in southern China during the period from 2013-2015. Sci. Rep. 7, 6576.

Feng, K.Y., Chen, T., Zhang, X., Shao, G.M., Cao, Y., Chen, D.K., Lin, W.C., Chen, F., Xie, Q.M., 2018. Molecular characteristic and pathogenicity analysis of a virulent recombinant avain infectious bronchitis virus isolated in China. Poult. Sci. 97, 3519–3531.

Gomaa, M.H., Barta, J.R., Ojkic, D., Yoo, D., 2008. Complete genomic sequence of turkey coronavirus. Virus Res. 135, 237–246.

Gong, L., Li, J., Zhou, Q., Xu, Z., Chen, L., Zhang, Y., Xue, C., Wen, Z., Cao, Y., 2017. A new Bat-HKU2-like coronavirus in swine, China, 2017. EMERG INFECT DIS 23.

Han, Z., Sun, C., Yan, B., Zhang, X., Wang, Y., Li, C., Zhang, Q., Ma, Y., Shao, Y., Liu, Q., Kong, X., Liu, S., 2011. A 15-year analysis of molecular epidemiology of avian infectious bronchitis coronavirus in China. Infect. Genet. Evol. 11, 190–200.

Huson, D.H., 1998. SplitsTree: analyzing and visualizing evolutionary data. BIOINFORMATICS 14, 68–73.

Ignjatovic, J., Galli, U., 1995. Immune responses to structural proteins of avian infectious bronchitis virus. Avian Pathol. 24, 313–332.

Jackwood, M.W., 2012. Review of infectious bronchitis virus around the world. Avian Dis. 56, 634–641.

Jackwood, M.W., Hilt, D.A., Callison, S.A., Lee, C.W., Plaza, H., Wade, E., 2001. Spike glycoprotein cleavage recognition site analysis of infectious bronchitis virus. Avian Dis. 45, 366–372.

Jiang, L., Zhao, W., Han, Z., Chen, Y., Zhao, Y., Sun, J., Li, H., Shao, Y., Liu, L., Liu, S., 2017. Genome characterization, antigenicity and pathogenicity of a novel infectious bronchitis virus type isolated from south China. Infect. Genet. Evol. 54, 437–446.

Kint, J., Fernandez-Gutierrez, M., Maier, H.J., Britton, P., Langereis, M.A., Koumans, J., Wiegertjes, G.F., Forlenza, M., 2015. Activation of the chicken type I interferon response by infectious bronchitis coronavirus. J. Virol. 89, 1156–1167.

Li, L., Xue, C., Chen, F., Qin, J., Xie, Q., Bi, Y., Cao, Y., 2010. Isolation and genetic analysis revealed no predominant new strains of avian infectious bronchitis virus circulating in South China during 2004-2008. Vet. Microbiol. 143, 145–154.

Li, Z., Wang, Y., Li, X., Li, X., Cao, H., Zheng, S.J., 2013. Critical roles of glucocorticoid-induced leucine zipper in infectious bursal disease virus (IBDV)-induced suppression of type I Interferon expression and enhancement of IBDV growth in host cells via interaction with VP4. J. Virol. 87, 1221–1231.

Liu, S.W., Zhang, Q.X., Chen, J.D., Han, Z.X., Liu, X., Feng, L., Shao, Y.H., Rong, J.G., Kong, X.G., Tong, G.Z., 2006. Genetic diversity of avian infectious bronchitis coronavirus strains isolated in China between 1995 and 2004. Arch. Virol. 151, 1133–1148.

Liu, X., Ma, H., Xu, Q., Sun, N., Han, Z., Sun, C., Guo, H., Shao, Y., Kong, X., Liu, S., 2013. Characterization of a recombinant coronavirus infectious bronchitis virus with distinct S1 subunits of spike and nucleocapsid genes and a 3' untranslated region. Vet. Microbiol. 162, 429–436.

Reddy, V.R., Theuns, S., Roukaerts, I.D., Zeller, M., Matthijnssens, J., Nauwynck, H.J., 2015. Genetic characterization of the belgian nephropathogenic infectious bronchitis virus (NIBV) reference strain B1648. Viruses 7, 4488–4506.

Sawicki, S.G., Sawicki, D.L., 1998. A new model for coronavirus transcription. Adv. Exp. Med. Biol. 440, 215–219.

Sjaak, D.W.J., Cook, J.K., van der Heijden, H.M., 2011. Infectious bronchitis virus variants: a review of the history, current situation and control measures. Avian Pathol. 40, 223–235.

Thor, S.W., Hilt, D.A., Kissinger, J.C., Paterson, A.H., Jackwood, M.W., 2011. Recombination in avian gamma-coronavirus infectious bronchitis virus. Viruses 3, 1777–1799.

Valastro, V., Holmes, E.C., Britton, P., Fusaro, A., Jackwood, M.W., Cattoli, G., Monne, I., 2016. S1 gene-based phylogeny of infectious bronchitis virus: an attempt to harmonize virus classification. Infect. Genet. Evol. 39, 349–364.

Wang, C.H., Huang, Y.C., 2000. Relationship between serotypes and genotypes based on the hypervariable region of the S1 gene of infectious bronchitis virus. Arch. Virol. 145, 291–300.

Wang, C.H., Tsai, C.T., 1996. Genetic grouping for the isolates of avian infectious bronchitis virus in Taiwan. Arch. Virol. 141, 1677–1688.

Wu, X., Yang, X., Xu, P., Zhou, L., Zhang, Z., Wang, H., 2016. Genome sequence and origin analyses of the recombinant novel IBV virulent isolate SAIBK2. Virus Genes 52, 509–520.

Xu, Q., Han, Z., Wang, Q., Zhang, T., Gao, M., Zhao, Y., Shao, Y., Li, H., Kong, X., Liu, S., 2016. Emergence of novel nephropathogenic infectious bronchitis viruses currently circulating in Chinese chicken flocks. Avian Pathol. 45, 54–65.

Xu, L., Han, Z., Jiang, L., Sun, J., Zhao, Y., Liu, S., 2018. Genetic diversity of avian infectious bronchitis virus in China in recent years. Infect. Genet. Evol. 66, 82–94.

Yang, J.T., Ma, B.C., 2013. Complete genome sequence of a nephropathogenic infectious bronchitis virus strain isolated in China. Genome Announc. 1.

Zhang, T., Han, Z., Xu, Q., Wang, Q., Gao, M., Wu, W., Shao, Y., Li, H., Kong, X., Liu, S., 2015. Serotype shift of a 793/B genotype infectious bronchitis coronavirus by natural recombination. Infect. Genet. Evol. 32, 377–387.

Zhang, Y., Huang, S., Zeng, Y., Xue, C., Cao, Y., 2018. Rapid development and evaluation of a live-attenuated QX-like infectious bronchitis virus vaccine. VACCINE 36, 4245–4254.